Electronic Supplementary Information

Template-directed synthesis of a luminescent Tb-MOF material for highly selective Fe^{3+} and Al^{3+} ions detection and VOC vapor sensing

Di-Ming Chen, Nan-Nan Zhang, Chun-Sen Liu* and Miao Du*

Henan Provincial Key Laboratory of Surface & Interface Science, Zhengzhou University of Light Industry, Zhengzhou 450002, Henan, China

Authors for correspondence: chunsenliu@zzuli.edu.cn; dumiao@zzuli.edu.cn

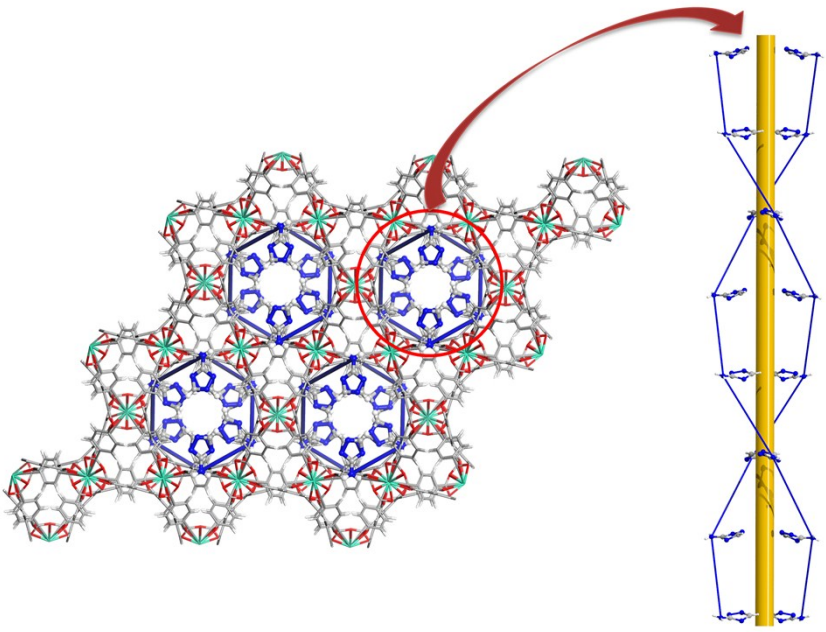

Fig. S1 View of the double-stranded helical chains formed by the Hatz ligands.

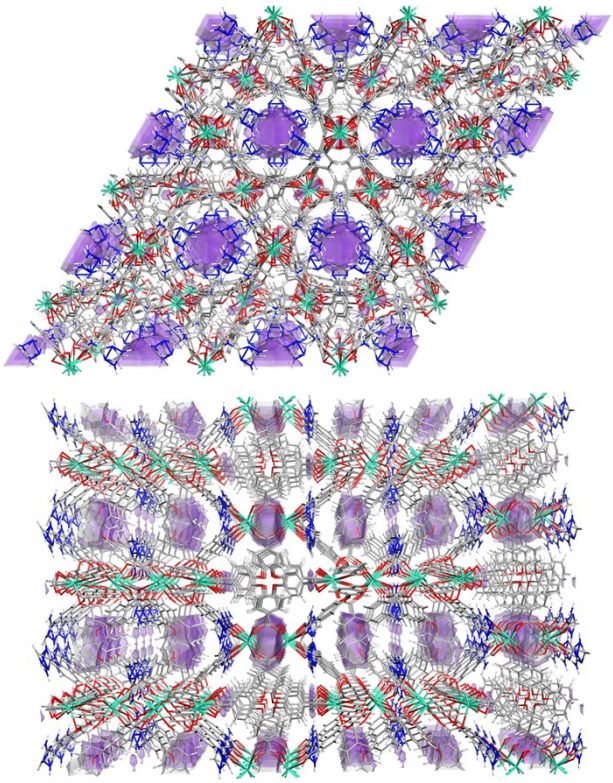

Fig. S2 View of the finite spaces partitioned by the Hatz ligands.

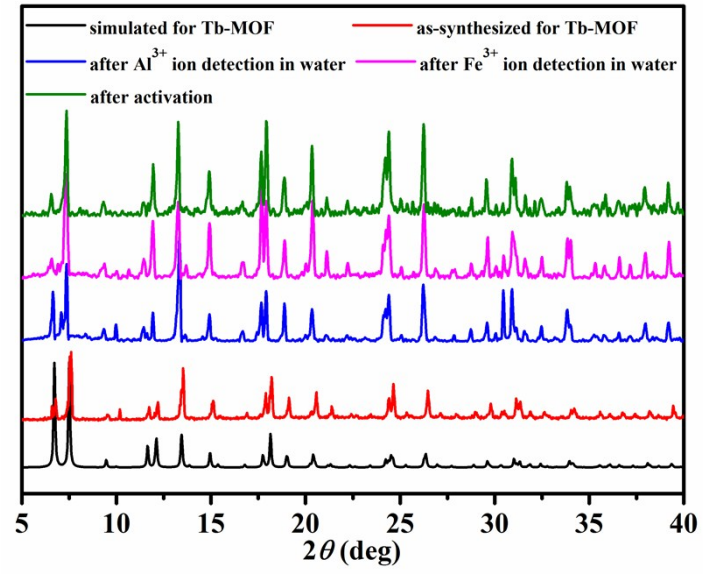

Fig. S3 PXRD patterns for the Tb-MOF and its derivatives.

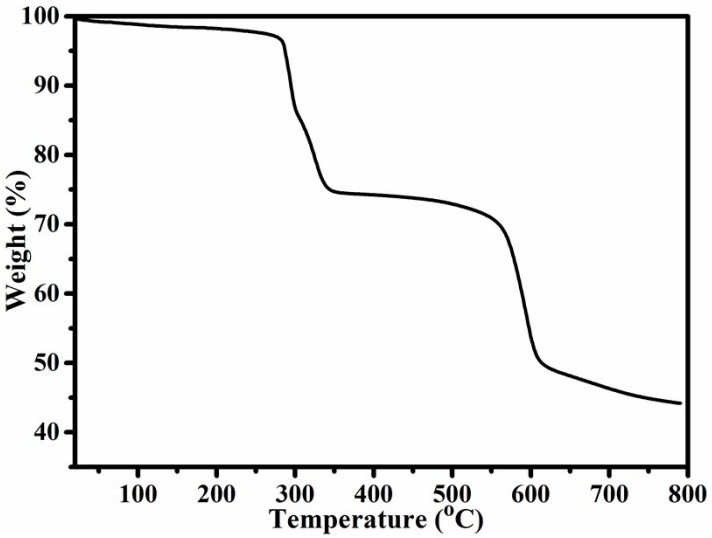

Fig. S4 TGA curve for the Tb-MOF.

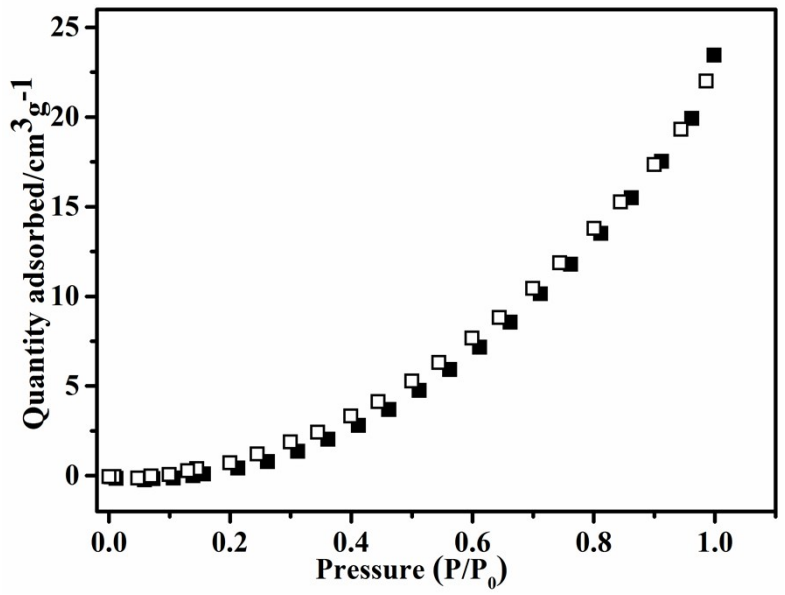

Fig. S5 N_2 sorption isotherm for the activated Tb-MOF at 77 K.

Calculation of sorption heat for CO_2 and C_2H_2 uptake using Virial fitting

$$\ln P = \ln N + 1/T \sum_{i=0}^{m} a_i N^i + \sum_{i=0}^{n} b_i N^i \qquad Q_{st} = -R \sum_{i=0}^{m} a_i N^i$$

The above virial expression was used to fit the combined isotherm data for **1a** at 273 and 298 K, where P is the pressure, N is the adsorbed amount, T is the temperature, a_i and b_i are virial coefficients, and m and N are the number of coefficients used to describe the isotherms. Q_{st} is the coverage-dependent enthalpy of sorption and R is the universal gas constant.

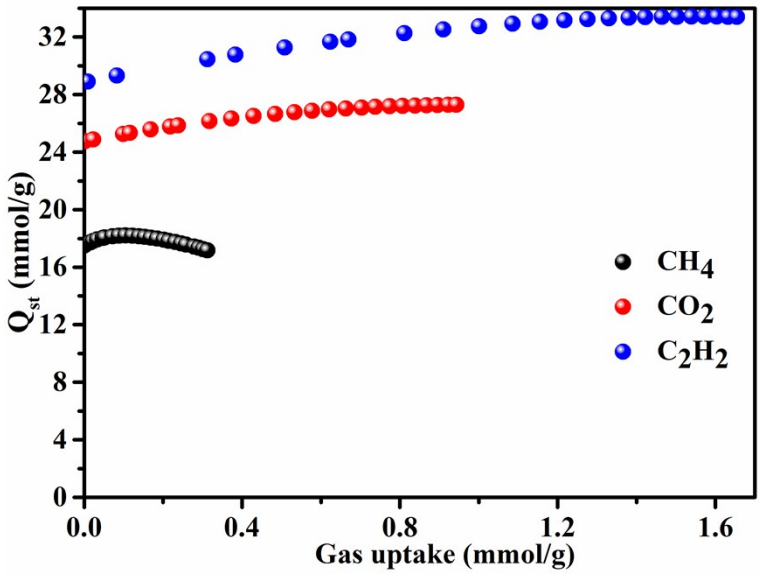

Fig. S6 Gas adsorption heats for the activated Tb-MOF.

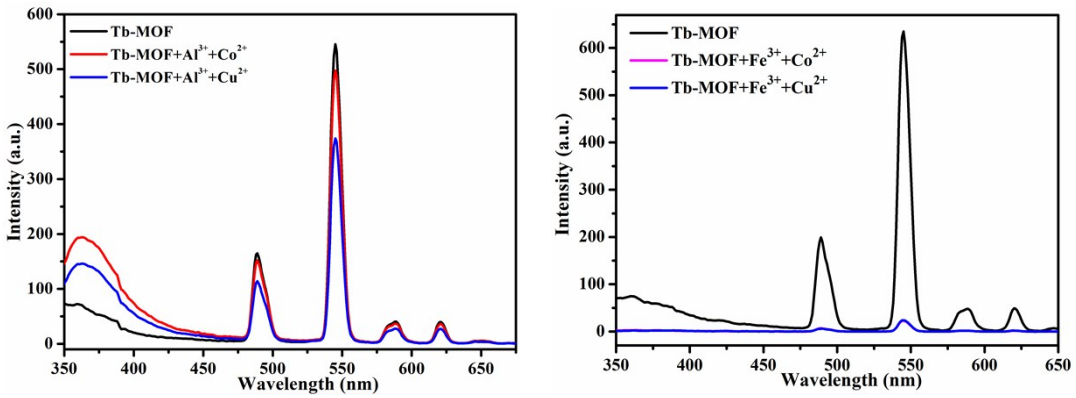

Fig. S7 The competition experiments for the detection of Fe^{3+} and Al^{3+} ions in the presence of Cu^{2+} or Co^{2+} ion.

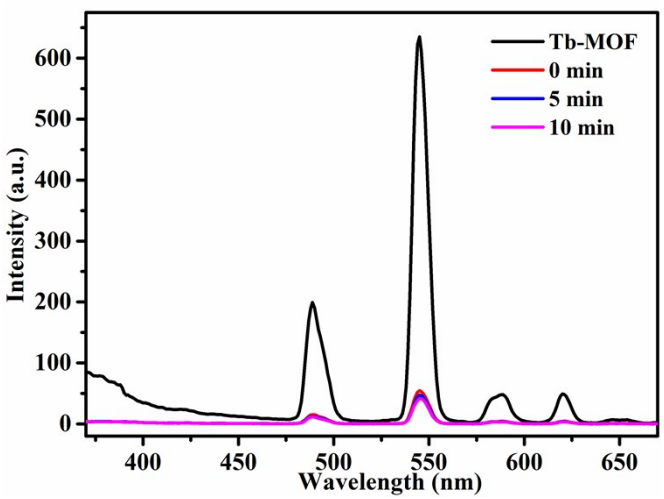

Fig. S8 Time-dependent emission spectra for the Tb-MOF in water containing 10^{-3} M Fe^{3+} ion.

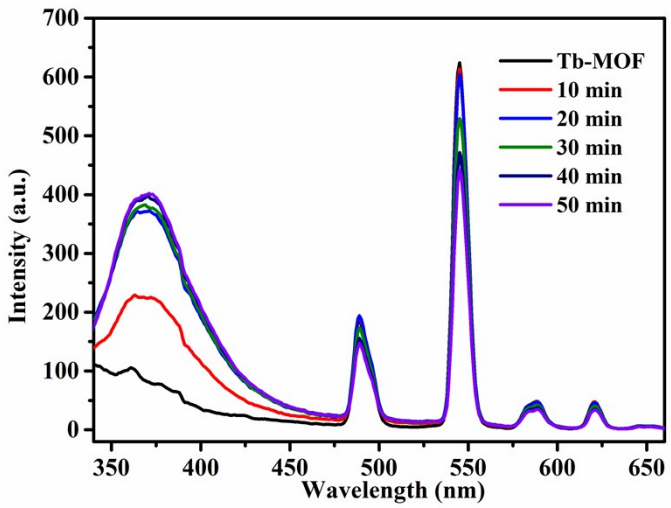

Fig. S9 Time-dependent emission spectra for the Tb-MOF in water containing 10^{-3} M Al^{3+} ion.

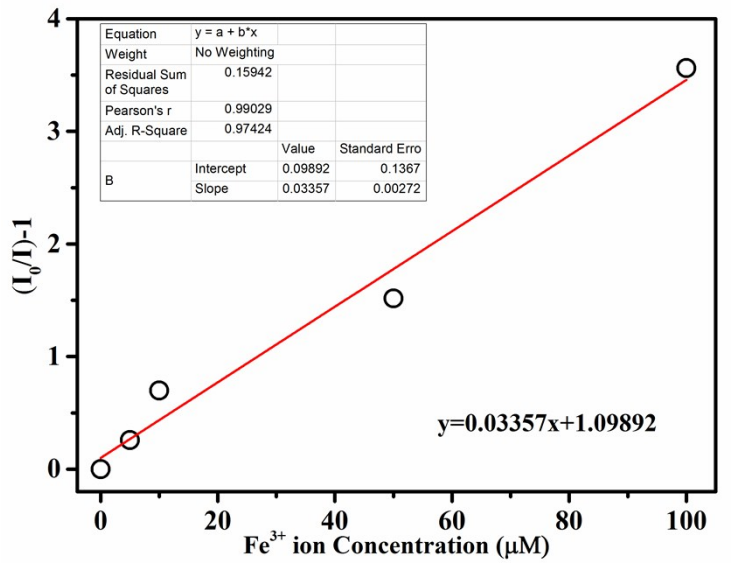

Fig. S10 K_{sv} curve of Tb-MOF in aqueous solutions in the presence of various concentrations of Fe^{3+} ion.

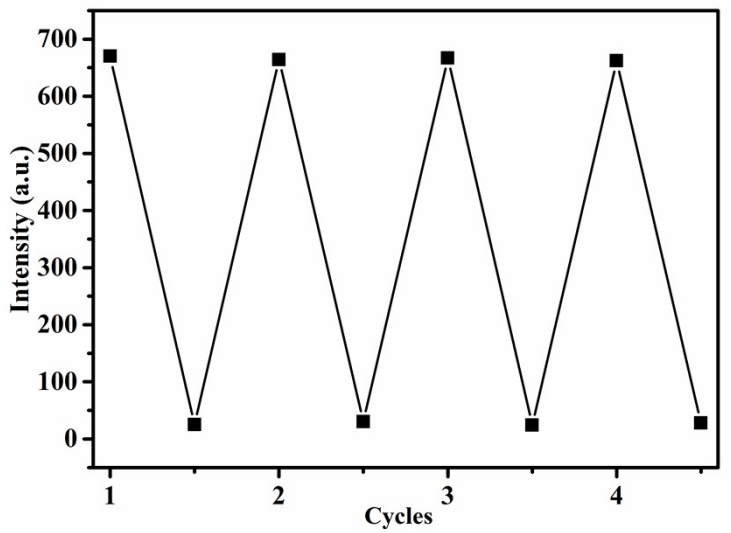

Fig. S11 The quenching and recovery tests of **1**.

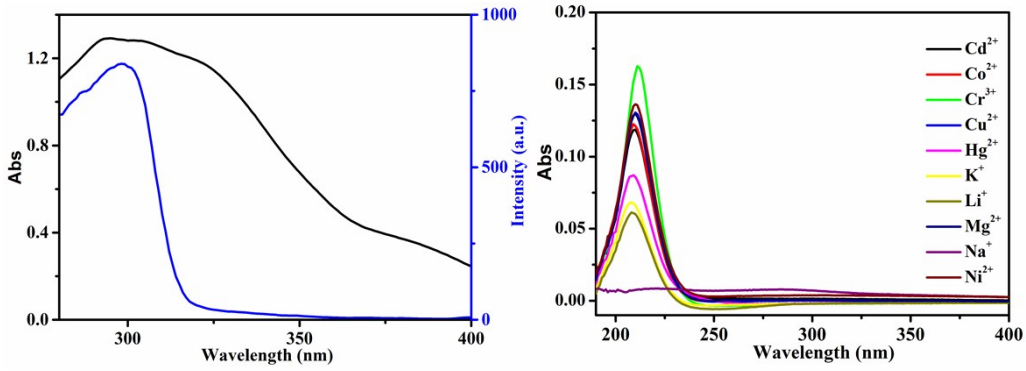

Fig. S12 Views for the UV adsorption spectrum of Fe^{3+} ion in water and exaction spectrum for the Tb-MOF (left) and the UV adsorption spectra of other metal ions used in the luminescent detection (right).

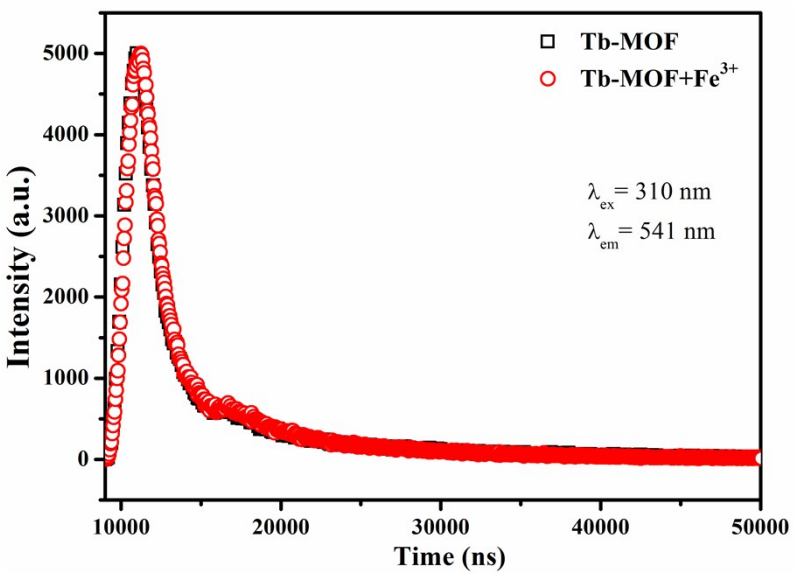

Fig. S13 Fluorescence decay profiles of Tb-MOF in the presence or absence of Fe^{3+} ion.

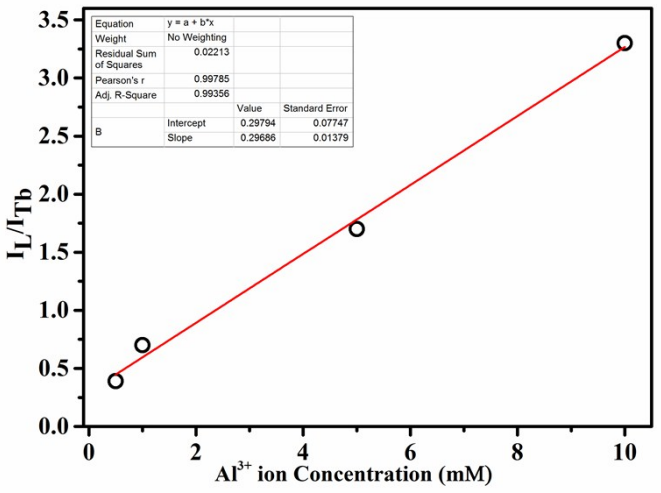

Fig. S14 Linear relationship of ration for the ligand-based and metal-based emission intensity *vs.* the concentration of Al^{3+} ion.

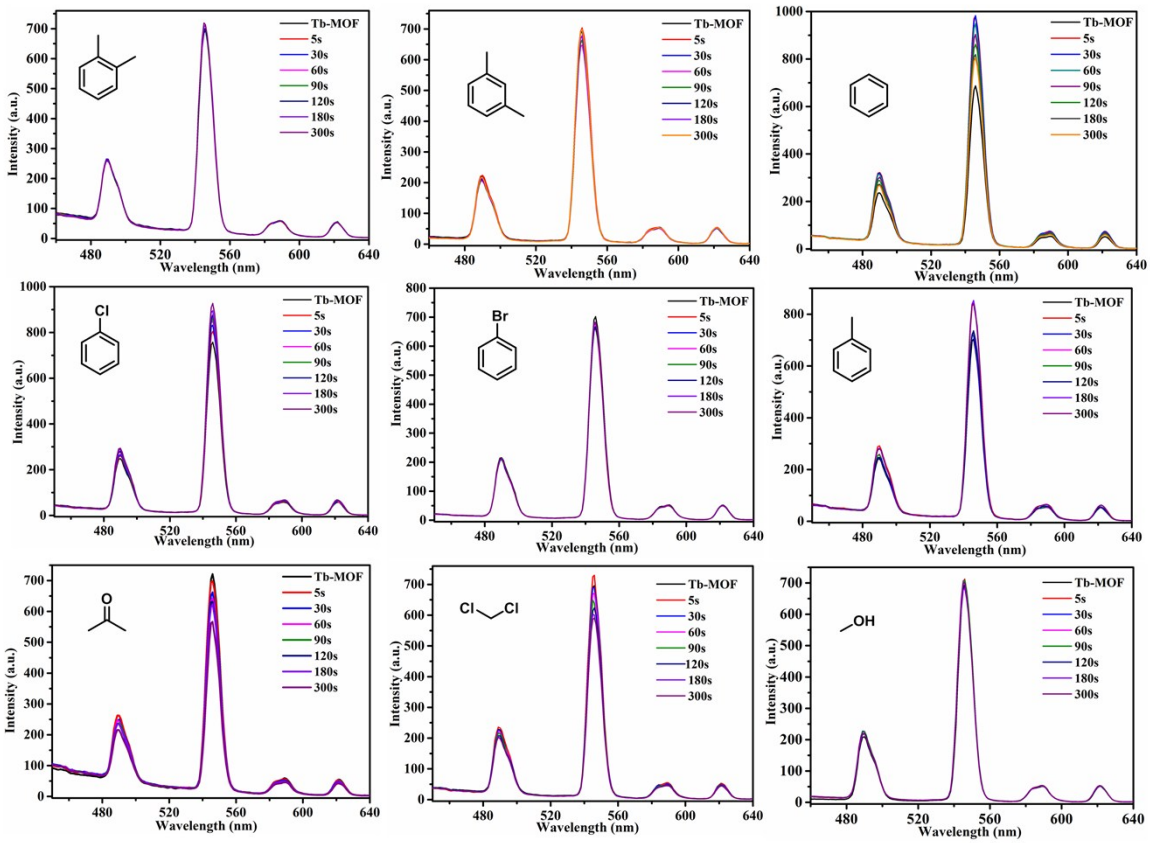

Fig. S15 Time-dependent emission spectra for the Tb-MOF in various VOC vapors.

Table S1 Crystal data and structure refinement details for Tb-MOF.

Empirical formula	$C_{32}H_{28}N_5O_{10}Tb$
Formula weight	801.51
Temperature / K	293(2)
Crystal system	hexagonal
Space group	$P6_422$
a / Å	15.1834(4)
b / Å	15.1834(4)
c / Å	26.5282(9)
α / °	90
β / °	90
γ / °	120
Volume / Å^3	5296.3(3)
Z	6
ρ_{calc} / g cm^{-3}	1.508
μ / mm^{-1}	2.063
F(000)	2400.0
Radiation	Mo Kα (λ = 0.7107)
Reflections collected	14753
Independent reflections	3121 [R_{int} = 0.0275, R_{sigma} = 0.0205]
Data/restraints/parameters	3121/46/242
Goodness-of-fit on F^2	1.124
Final R indexes [I >= 2σ (I)]	R_1 = 0.0381, wR_2 = 0.1045
Final R indexes [all data]	R_1 = 0.0456, wR_2 = 0.1120
Largest diff. peak and hole / e Å^{-3}	1.03 and -0.62
Flack parameter	-0.003(8)